



MARCH 16, 2023

APPLICATIONS OF LIDAR IN PREDICTING
MEAN ANNUAL SUSPENDED SEDIMENT
YIELD IN A MOUNTAIN CATCHMENT

CE 513: GIS IN WATER RESOURCES FINAL REPORT

ZACHARY PERRY

Project Website: web.engr.oregonstate.edu/~perryz/



Table of Contents

Table of Figures.....	1
Abstract.....	2
Background.....	2
Study Site.....	3
Objectives.....	5
Methods and Processing.....	6
Results.....	13
Conclusions.....	16
Next Steps.....	16
Data Sources.....	17
References.....	17

Table of Figures

Figure 1: A map of the HJ Andrews Experimental Forest.....	3
Figure 2: A map of the geology at the HJ Andrews Experimental Forest	4
Figure 3: Experimental watersheds at the HJ Andrews Experimental Forest	5
Figure 4: Workflow for watershed delineation.....	6
Figure 5: Flow direction errors due to road network.....	7
Figure 6: Workflow for watershed delineation with resampling.....	7
Figure 7: Stream network derived for the HJ Andrews Experimental Forest	8
Table 1: Ungauged watershed descriptions.....	8
Figure 8: Pour point issues in watershed delineation.....	9
Figure 9: Manually adjusting a watershed.....	10
Figure 10: Results of the change analysis.....	11
Figure 11: Hydrologic data for linear modelling.....	12
Figure 12: Delineated watersheds.....	12
Figure 13: Delineated watersheds and experimental watersheds over a hillshade.....	13
Table 2: Comparing metrics derived from different DEMs.....	13
Table 3: Topographic metrics for the experimental watersheds.....	14
Table 4: Sample modelling results using multiple linear regressions.....	14
Table 5: Topographic metrics for ungauged basins.....	15
Table 6: Results of predictions of mean annual suspended sediment yield.....	15

Abstract

The influence of landscape, geologic history, and geomorphic disturbance legacies can have a large impact on streamflow characteristics in mountain catchments. While it can be difficult to elucidate subsurface catchment properties using LiDAR, past studies have shown that measurable topographic indices like surface roughness can reflect relative differences in unconsolidated colluvium and soil depth. The HJ Andrews Experimental Forest (HJA) provides a unique opportunity to explore how physiography influences streamflow because within its borders lay a wide range of catchment types and sizes. The geologic history of the HJA is well documented through multiple historical surveys and streamflow data has been collected at numerous experimental watersheds for decades. This rich dataset, combined with the unique physiographic characteristics of the region, make for easy comparisons between catchments. Here we seek to determine if mean annual suspended sediment yield (SSY) can be estimated using metrics of topography and erosion rate as measured by LiDAR in 10 experimental catchments. Our analysis found that while there is a relationship between some of our metrics and mean annual SSY, linear models alone cannot make accurate predictions at all scales. Using these models, we predicted mean annual SSY in 4 ungauged basins characterized by different terrain and geomorphic disturbance legacies. Larger catchment (>5km²) predictions were more accurate with all models tested. The results suggest a need for further analysis with a wider range of catchment sizes and a way to quantify landscape and climate disturbance legacies.

Background

Headwater streams are critically important for the health of downstream ecosystems. Sediment in these streams provides habitat for many freshwater faunas, such as salmon and salamanders. The size of the sediment load can greatly impact the ability of these creatures to spawn. Salmon, for example, only lay eggs in beds with specific size distributions of sediment. Any disruption to these already sensitive populations could prove disastrous for local biodiversity. Sediment supply also works to shape downstream channel morphology, shaping the rivers we all know so well. They may look the same day by day, but at larger time scales, their shapes are dynamic.

Looking at sediment yield at the headwater scale can be difficult because the variability can often be extremely high from year to year. Yet it is still valuable to have an estimate of what these small catchments may produce in an average year. Since rivers are the sum of headwaters, understanding the sediment production processes in these small systems will also work to educate us about the inputs to larger rivers.

LiDAR technology has evolved rapidly over the past few decades. Aerial surveys using this technology have proven to be a useful tool for answering various questions regarding sediment load and yield at different scales (Pavelsky and Smith, 2009; Anderson and Pitlick). Change analysis is a tool that is often used to determine how landscapes have changed through time (DeLong et al., 2022). By integrating high resolution LiDAR from two different acquisitions, 12 years apart, we hope to use change analysis as a means of predicting relative erosion rate in a given catchment.

Previous studies have shown a connection exists between topography, discharge, and suspended sediment yield (Bywater-Reyes et al., 2018) in small mountain catchments. Building on this

analysis, we will seek to determine if metrics derived entirely from LiDAR can be used to make predictions of SSY in the same mountain catchments.

Study Site

The HJ Andrews Experimental Forest is a research forest located in the Western Cascade Mountains of Oregon. It makes up the entirety of the Lookout Creek Watershed (64km²) and empties into Blue River Reservoir, which drains to the McKenzie River (Fig 1).

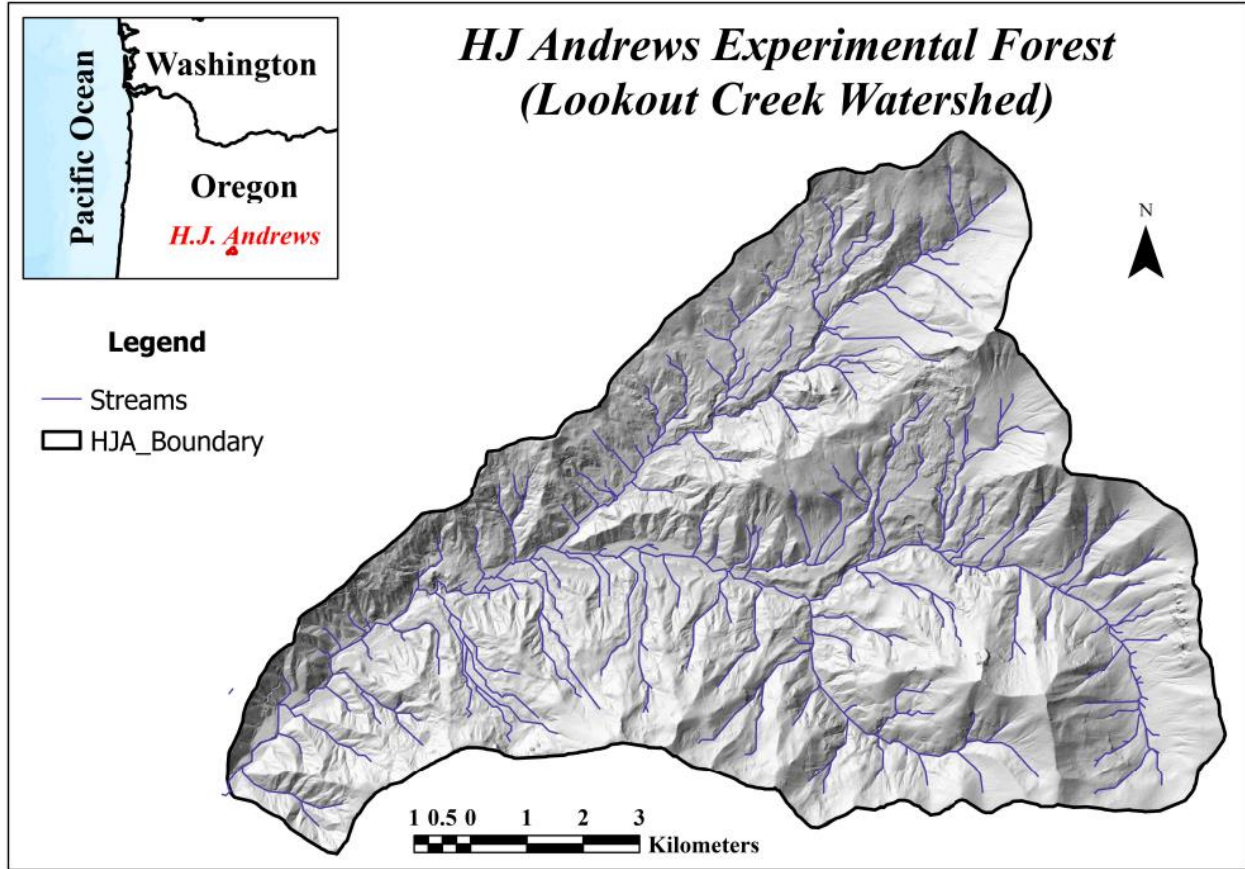


Fig 1. A map of the HJA with the stream network and outer boundary highlighted.

Lookout Creek is a 5th order stream and drains a 64km² catchment. The climate of the region is Mediterranean, characterized by dry, hot summers and cool, wet winters. The Andrews Forest is made up of primarily Old-growth trees: Douglas-fir (*Pseudotsuga menziesii*) and western hemlock (*Tsuga heterophylla*) at lower elevation and noble fir (*Abies procera*) and Pacific silver fir (*Abies amabilis*) at upper elevations. The elevation gradient is steep (430->1600m.a.s.l) and the terrain is marked by both steep, V-shaped valleys and large, U-shaped valleys carved out by glaciation. The region is underlain by volcanic bedrock, which can be separated into 3 distinct periods (Fig 2).

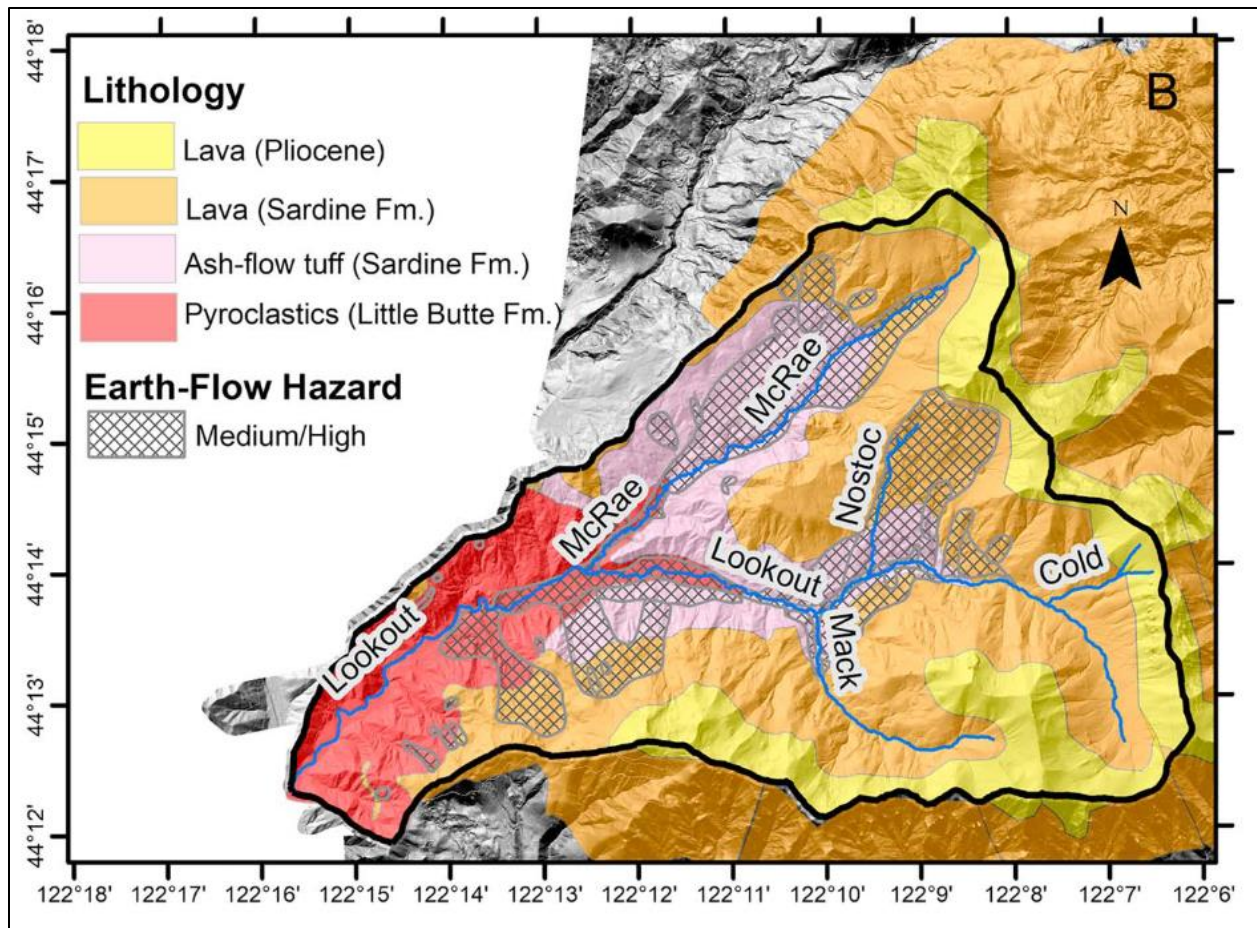


Fig 2. A map illustrating the geologic history of the HJA (Swanson, 2005).

In the lowest elevations (Little Butte Fm.) lays the oldest bedrock. It is composed of highly weather pyroclastics and ash-flow tuffs. The middle elevations (Sardine Fm.) are composed of a layer of ash-flow tuffs and a layer of lava flows. This elevation is significantly less weathered than the lower region. The highest elevations (Pliocene) are underlain by lava flows and forms a thick cap of porous basalt on the ridgelines.

Established in 1948, the forest was meant to improve our understanding of how different logging practices influence old growth forests and headwater stream hydrology. Ten experimental watersheds were established, and experiments were carried out.

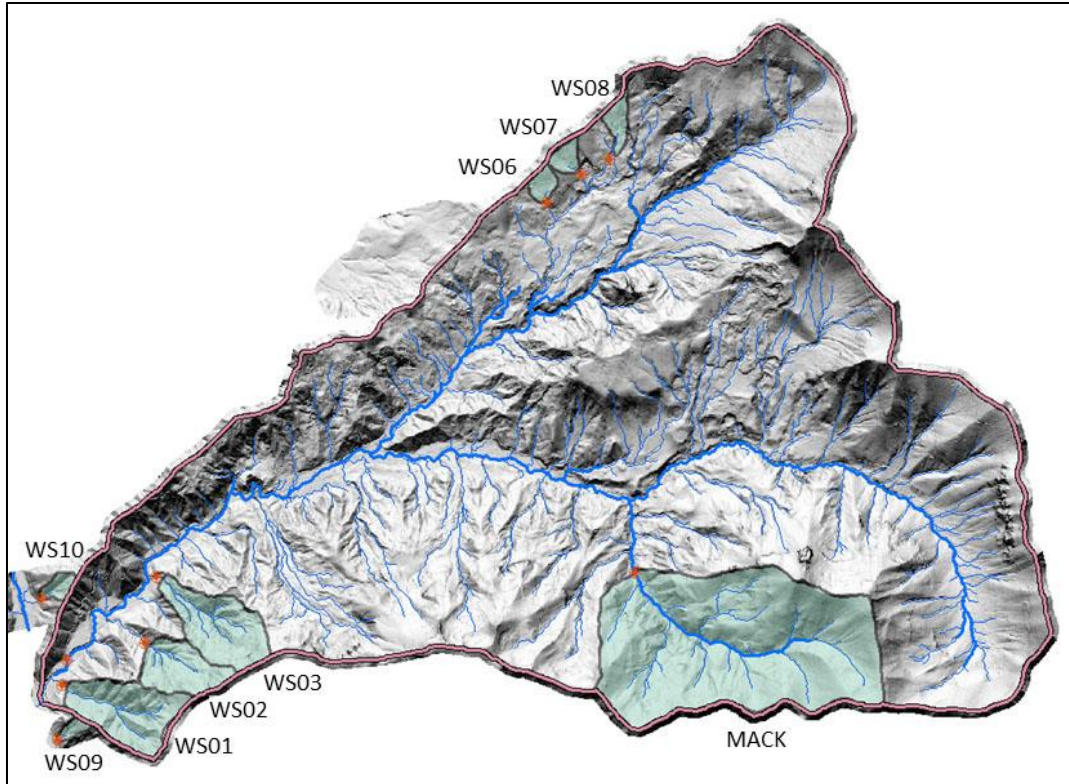


Fig 3. The ten experimental watersheds established by the HJA to study the impacts of logging.

In 1980, the site became a charter member of the NSF funded Long Term Ecological Research (LTER) Network. The region has been impacted by many large disturbances throughout the past 8 decades. Two major floods in 1964 and 1996 wreaked havoc on HJA infrastructure and moved enormous amounts of sediment and large wood, triggering many debris slides and flows. In 2020, the Holiday Farm Fire touched the edges of the forest, burning parts of the lower experimental watersheds.

Ongoing work at the HJA focuses on interactions between different parts of the forest (climate, hydrology, ecology, disturbance impacts). The region was mapped with aerial LiDAR in 2008 and 2020, generating bare Earth Digital Elevation Models (DEM) for each data acquisition (1m resolution).

Objectives

1. Utilize ArcGIS Pro to create shapefiles for the watersheds of interest using watershed delineation workflow.
2. Use zonal statistics to extract topographic and hydrologic metrics from each watershed.
3. Evaluate the difference in data derived from DEMs created using LiDAR collected in 2008 and 2020.
4. Utilize change analysis to calculate change in elevation as a proxy measure of relative erosion rate.
5. Utilize linear regression modelling to determine if measures of topography and relative erosion rates can estimate the spatial variability in mean annual suspended sediment yield.

Methods and Processing

This analysis relied heavily on ArcGIS Pro tools to develop shapefiles for previously ungauged and unmeasured basins in the HJA. To create the shapefile, the DEM of elevation created from the 2020 flight acquisition (hereafter DEM20) was uploaded to GIS. DEM20 was chosen for watershed delineation because it has a much higher point cloud density than the DEM created in 2008 (hereafter DEM08). Fig 4 shows the steps that were applied to the DEM and resulting rasters to delineate the watersheds of interest.

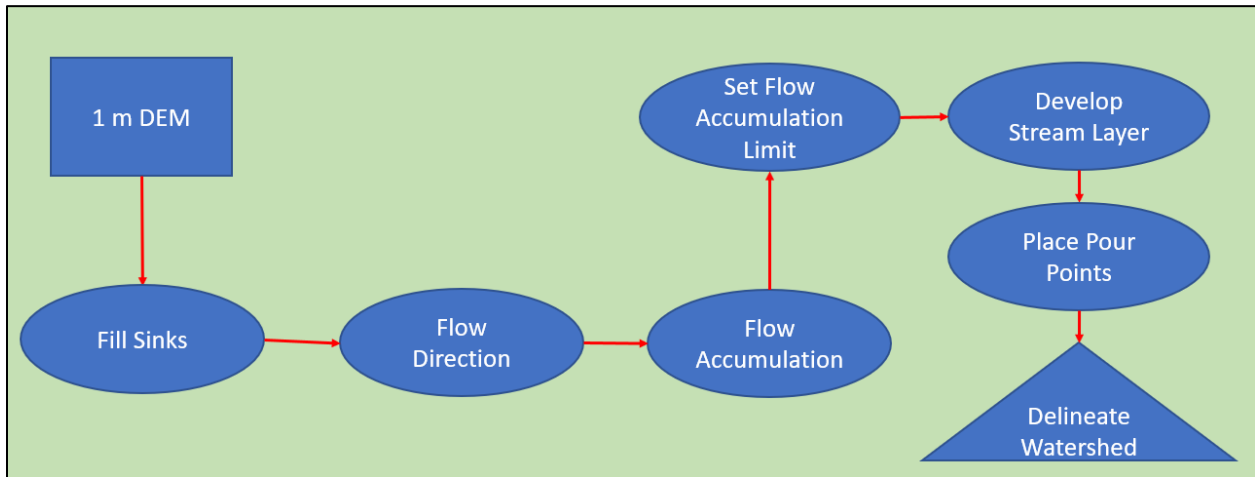


Fig 4. Steps used in ArcGIS Pro to delineate watersheds.

However, this processing failed to successfully delineate any watersheds. The issue stems from the road network present at the HJA, which at 1m resolution is assumed to be a flow path for water by GIS (Fig 5). This resulted in flow accumulation lines flowing down the roads, contrary to reality. The roads at the site were built with good drainage and frequent sluice pipes. They are also built with a slight slope so that water continues flowing over them and down the hillslope.

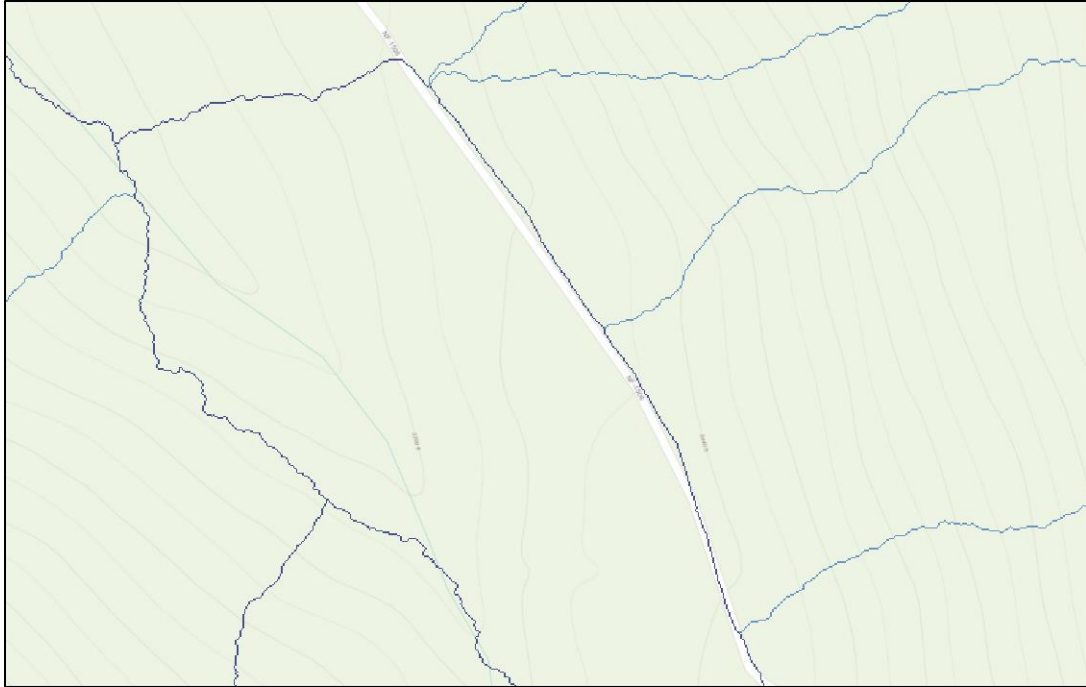


Fig 5. This snapshot highlights how the roads led to artificial rivers being formed by GIS software.

To navigate this issue, a resampling was completed on the DEM to see if a coarser resolution would remove the influence of the roads while retaining general valley and terrain characteristics to still delineate watersheds. This was completed for 5, 10, 20 and 30m. The 30m resolution DEM was found to have a good balance of meeting these two objectives. Fig 6 shows the new steps used to delineate the watersheds.

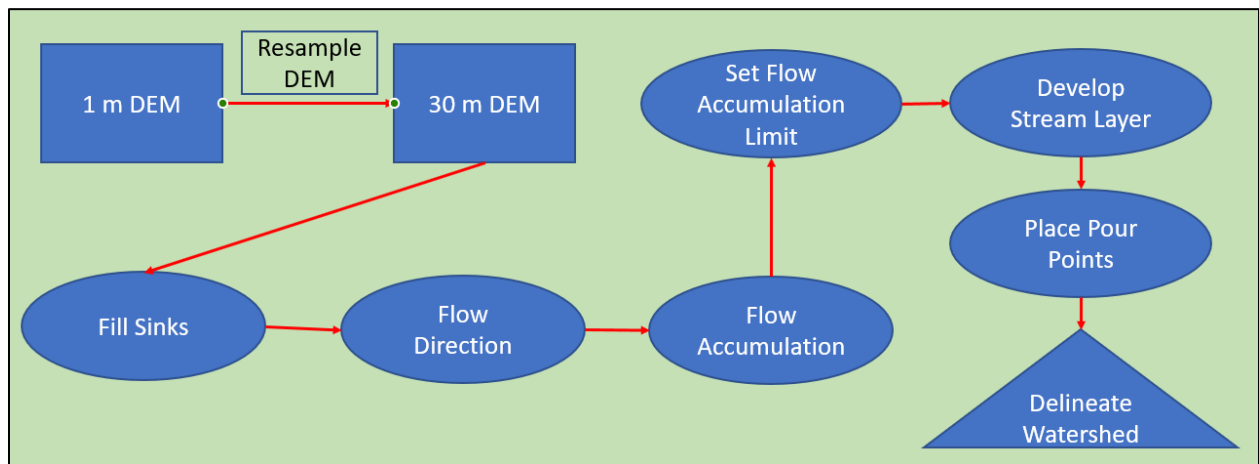


Fig 6. Steps used in ArcGIS Pro to delineate watersheds and avoid the artificial influence of roads.

Aside from resampling the data, the other step that required fine tuning was setting the flow accumulation limit. Values spanning a long range were tested until the streams generally lined up with our field knowledge of the site and the original stream layer developed with DEM08. The

original stream layer could have been used for this analysis, but it has a few glaring errors where it has placed streams in the wrong location. In general, it is a good reference and was an easy way to assess the new stream layer, shown in Fig 7.

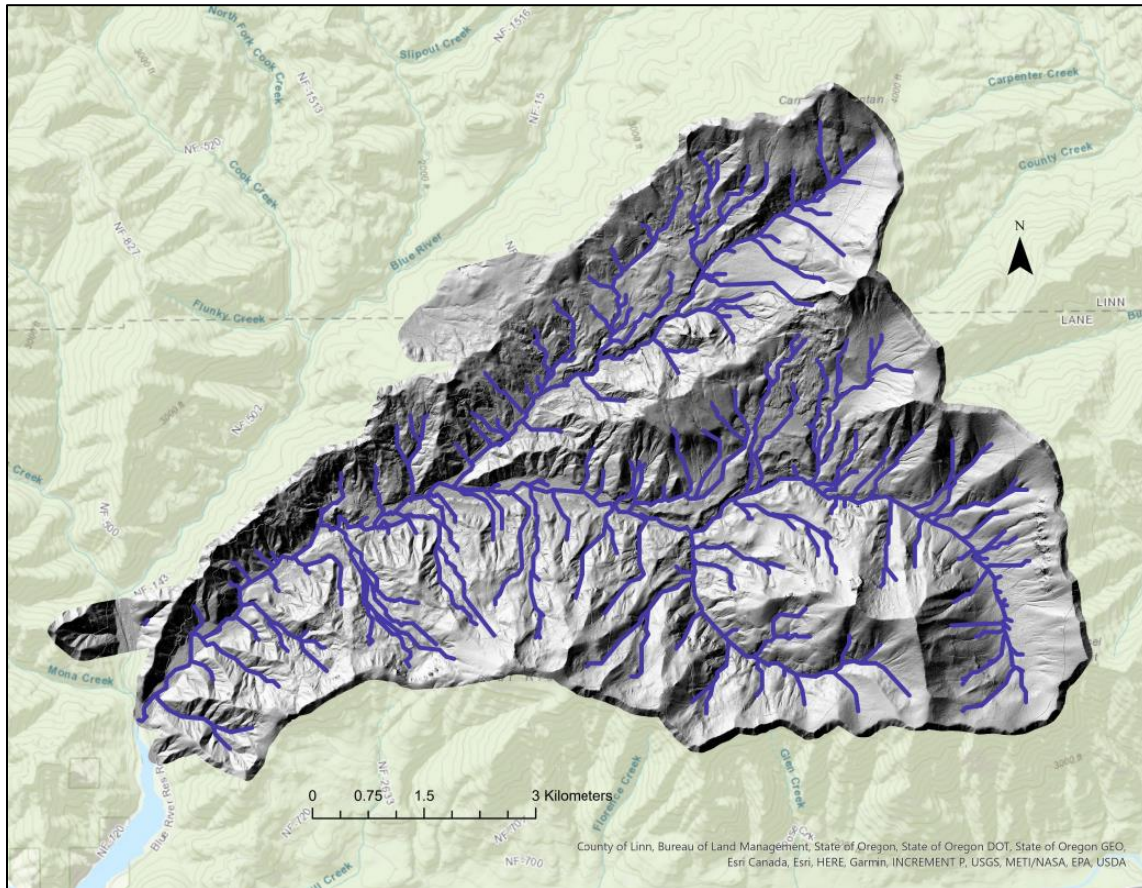


Fig 7. The stream layer created as part of the watershed delineation process in the HJA.

There are four primary watersheds of interest in this catchment that were up to this point, never delineated: McRae Creek, Cold Creek, Longer Creek, and Nostoc Creek. These creeks are of much interest to our research group as they all have very different characteristics, as outlined in Table 1.

<u>Watershed</u>	<u>Order</u>	<u>Vegetation</u>	<u>Geology</u>	<u>Topography</u>
McRae Creek (MC)	4 th order stream	Primarily old growth, some legacy harvesting in small patches	Ash-flow tuffs and lava flows, unglaciated	Variable slope, thick colluvial deposits
Longer Creek (LC)	3 rd order stream	Old growth	Ash-flow tuffs and lava flows, drains to glaciated valley	Variable slope, drains active Earthflow

Nostoc Creek (NC)	3 rd order stream	Primarily old growth, some legacy harvesting in patches	Ash-flow tuffs and lava flows, glaciated	Variable slope, drains long, inner ridge
Cold Creek (CC)	2 nd order stream	Old growth	Lava flows, drains to glaciated valley	Steep slope, spring fed perennial stream

Table 1. Watersheds that we are trying to delineate and their characteristics.

Two of these watersheds (CC, LC) performed well in their delineations. Nostoc Creek had one problem. If the pour point was placed too close to the confluence of the stream with Lookout Creek, it delineated the watershed to include upstream Lookout. Instead, the pour point was moved upstream until a close approximation of drainage area was achieved. This is highlighted in Fig 8, where the large white delineation is the entirety of upper lookout upstream of Nostoc Creek. The light green delineation is the approximation of Nostoc after moving the pour point.

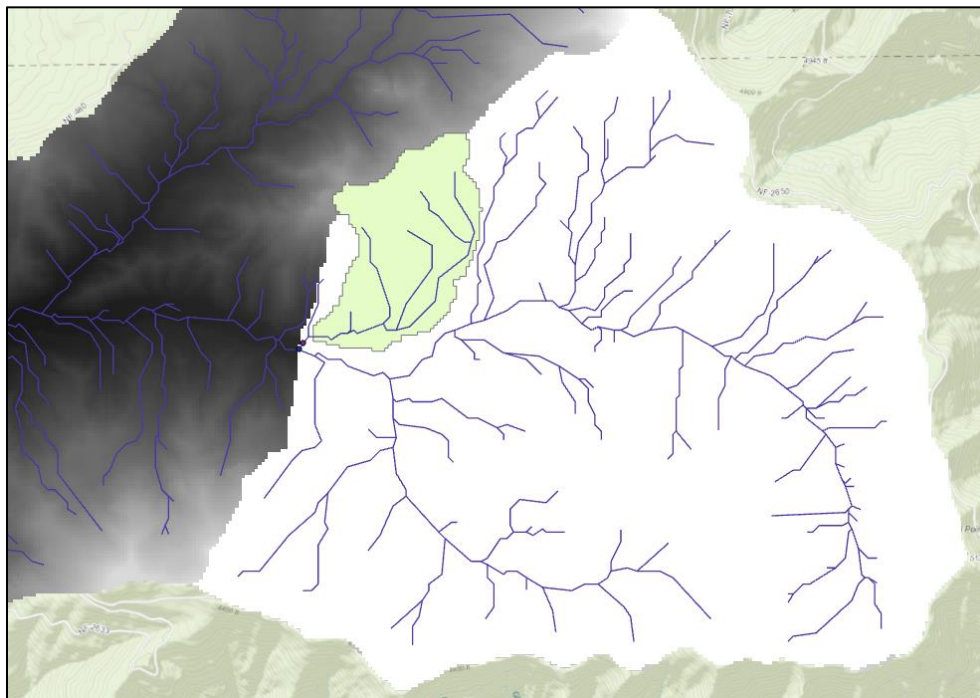


Fig 8. Two delineations overlaid on the HJA DEM. These were both produced by placing a pour point closer to the confluence of Lookout Creek (white) and further upstream Nostoc Creek (green).

Once the approximation was produced, the vertices were editing manually by following the contours to complete the delineation (Fig 9).

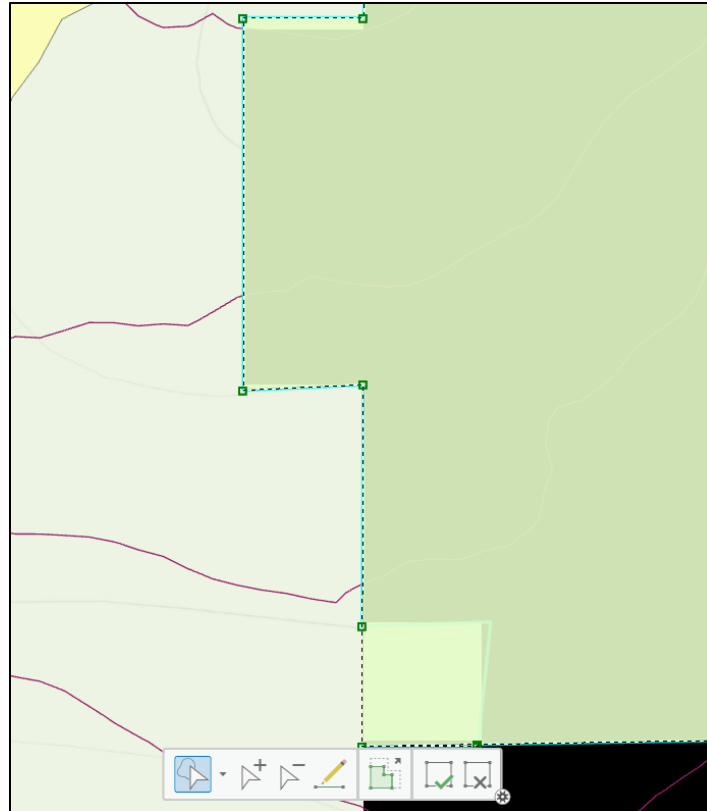


Fig 9. Manually editing shapefile vertices in GIS to complete the watershed delineation of Nostoc Creek.

These steps allowed a complete delineation of three of the watersheds (LC, NS, CC). McRae Creek failed to produce a watershed no matter where the pour point was placed. It is unclear what was leading to the failure of the GIS tool. Instead of automatic delineation, we are including a version of McRae delineated manually using a 10m contour from previous work. Finally, we added in the shapefile containing experimental watershed catchments and combined the shapefiles into a single file.

Topographic wetness index (TWI) was calculated across the rasters as well. TWI is a measure of steady-state wetness and is calculated with the following equation:

$$TWI = \ln(SCA/\tan b)$$

Where SCA is the specific catchment area, or the contributing area per unit contour, and b is the slope in radians. We hope TWI will provide a topographic metrics with hydrologic ramifications, providing information about how much of the rock surface is subjected to erosion by the forces of water movement.

To estimate relative erosion rate in each catchment, raster calculations were used to subtract DEM20 from DEM08. The resulting raster contained the difference in elevation at each cell. The literature suggested that anything under $\sim 2\text{m}$ was within error for LiDAR in a forested catchment (Edson and Wing, 2015). Everything less than 2m was given a value of zero, leaving total loss in

elevation at every cell in the raster. An example of a location where there was loss is shown in Fig 10.

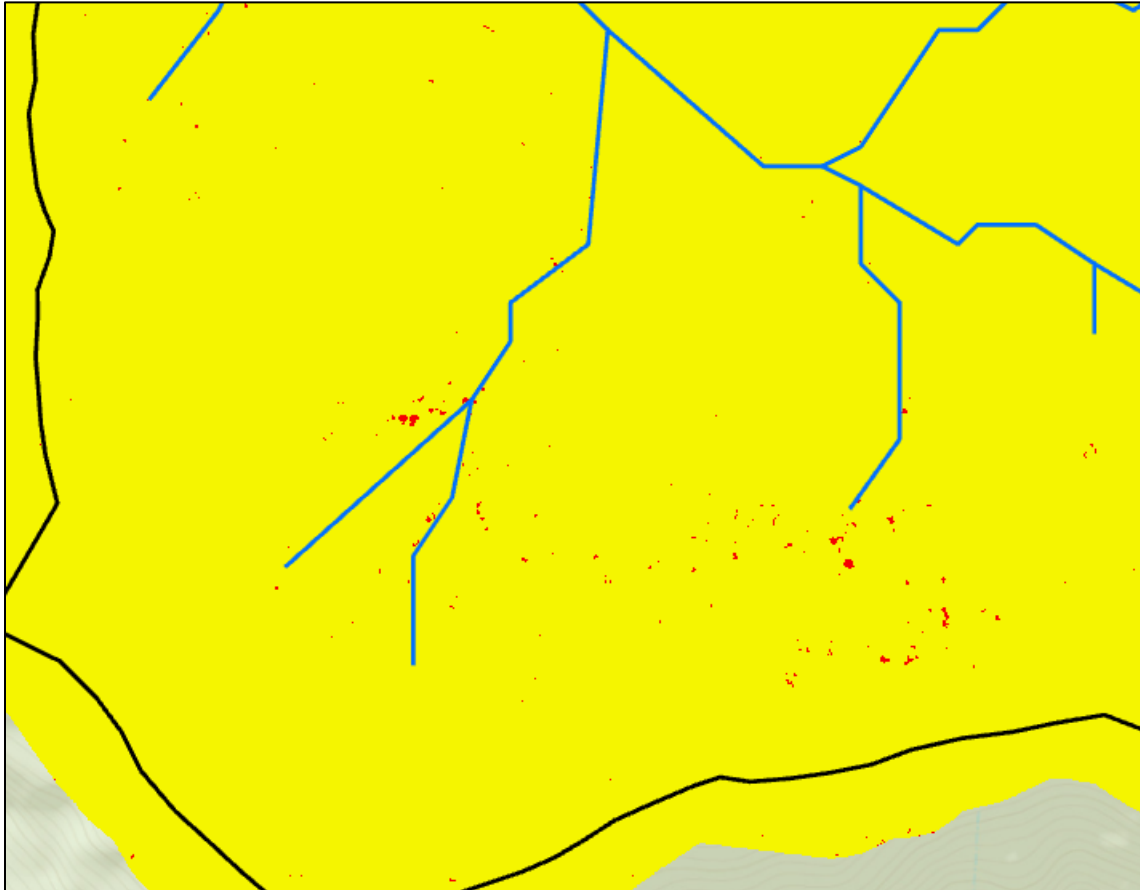


Fig 10. The results from the change analysis in a section of Mack Creek, showing loss of elevation in red.

The last step in ArcGIS was to extract our topographic and erosion rate metrics. The provided raster files containing slope and aspect were added. Zonal statistics were used to extract metrics from each catchment, as determined by the shapefile. This was performed with raster files and TWI calculations from the 2008 and 2020 LiDAR acquisitions as well as the raster of change in elevation.

Once the metrics were extracted for each watershed, they were evaluated using linear regression models to determine the best model for predicting mean annual SSY. The data used for this part of the analysis is shown in the Fig 11 (see data sources for more information). The metrics were also compared between DEM08 and DEM20 to see how they differ. This portion of the analysis was completed in Microsoft Excel.

<i>Mean and Standard Deviation of Annual Suspended Sediment Yield at Each Site Using All Annual Yields, Showing Number and Type of Suspended Sediment Samples per Site^a</i>					
Site	Mean annual sediment yield (t/km ²)	Median annual sediment yield (t/km ²)	Standard deviation (t/km ²)	SSC sample count	Sampling type
LOOK	231.3	147.9	141.8	136	Composite
MACK	67.7	31.9	17.0	420	Composite
WS01	97.1	48.0	205.5	1179 (976/203)	Storm-based/Composite
WS02	17.7	12.7	5.1	1278 (902/376)	Storm-based/Composite
WS03	108.2	42.7	2.2	1009	Storm-based
WS06	5.5	4.1	5.3	320	Composite
WS07	2.8	2.1	2.7	330	Composite
WS08	5.3	3.7	8.2	406	Composite
WS09	3.3	2.1	177.9	348	Composite
WS10	10.3	7.7	111.3	417	Composite

Fig 11. The suspended sediment data used for the linear model analysis (Bywater-Reyes et al., 2018).

Results

The results of the delineations for LC, NC, CC, and MC are shown in Fig 12 and the four new watersheds combined with the old shapefile is shown in Fig 13. The latter figure also shows a starker hillshade, to highlight the elevation gradient between and within the catchments.

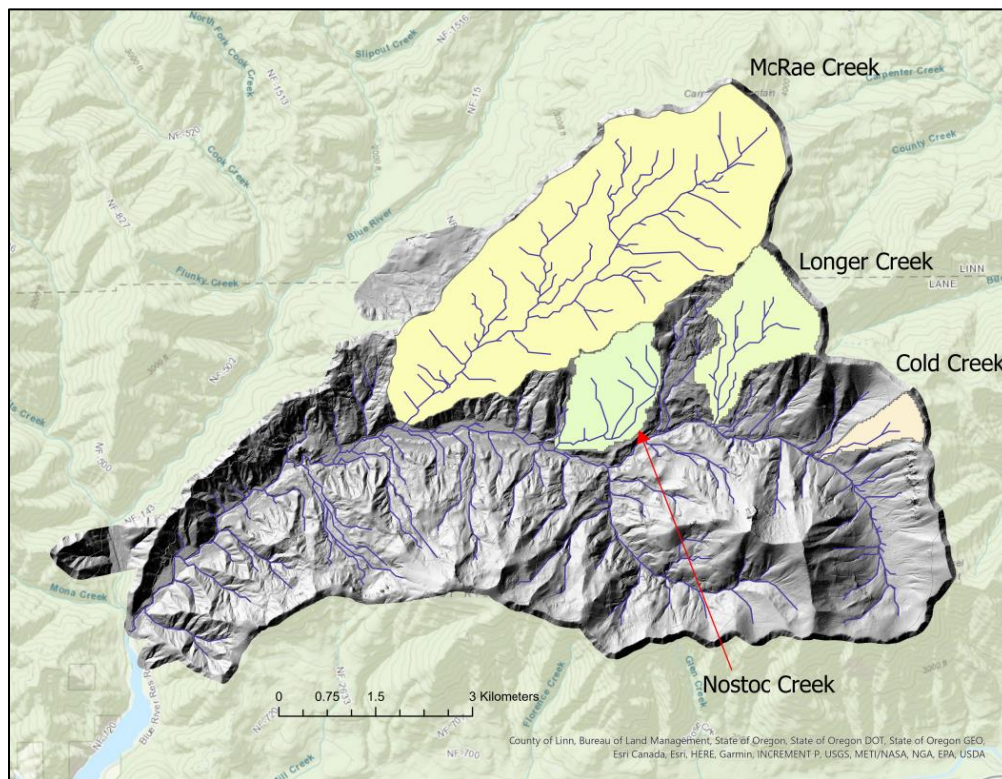


Fig 12. The results of the four watershed delineations in the HJA.

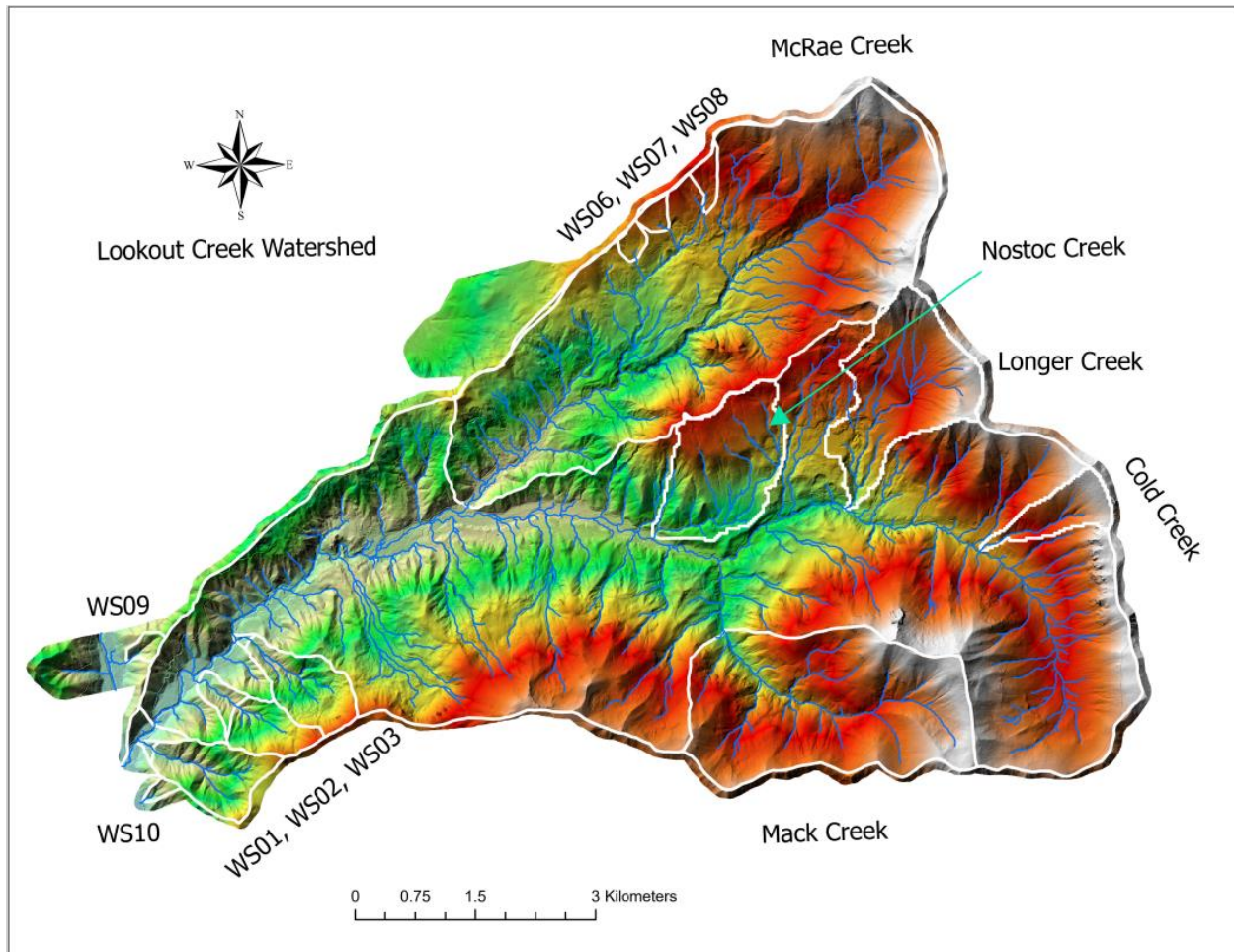


Fig 13. A map showing all catchments of interest, with elevation gradient shown in a hillshade (red = highest points, white = lowest).

Most of our work in the past has been completed using metrics derived from DEM08. The recent addition of DEM20 to our toolbox begs the question: how much do the DEMs differ? Table 2 below shows the results of correlating the metrics between each DEM.

<u>Metrics</u>	<u>R²</u>
Slope	0.999
Surface Roughness	0.998
Drainage Area	1.00
Topographic Wetness Index	0.987
Mean Elevation	1.00

Table 2. Topographic metrics derived from two DEMs were compared to see how much variance existed between the two models.

All of our metrics were almost a 1:1 match between the two DEM data sources. For the purposes of this analysis, this is close enough to assume the DEMs both provide a good assessment of topographic metrics. For the remainder of this analysis, metrics from DEM20 will be utilized. The metrics used for the linear modelling are shown in Table 3. These were tabulated for

watersheds feeding into the linear model – the HJA experimental watersheds. The final column, the sum of the change in elevation ($\Sigma\Delta z$), is the result of the change analysis – our proxy measure of relative erosion rate.

Watershed	Drainage Area (m ²)	Z Mean (m)	Slope Mean	Slope Std Dev (Roughness)	Mean TWI	Max TWI	$\Sigma\Delta z$ (m)
1	1011651	708	33.17	8.97	5.37	12.64	362
2	799592	748	31.75	9.63	5.61	12.63	259
3	954529	763	31.16	11.26	5.63	16.33	0
6	120071	948	17.13	6.47	6.23	9.73	0
7	124146	1003	18.17	6.07	6.19	9.56	17
8	160320	1075	20.1	8.87	6.19	10.4	2
9	71629	558	34.45	5.23	5.62	8.74	18
10	114454	592	32.15	8.44	5.22	8.96	12073
Mack	5786605	1193	27.47	9.27	5.9	14.5	76860
Lookout	62403044	979	24.42	11.18	6.18	19.48	362

Table 3. Topographic metrics and proxy erosion rate for each experimental watershed.

The results of the linear modelling are shown in Table 4. A selection of model setups is shown, but in total over 20 variable combinations were analyzed.

Model #	Y	X1	X2	X3	R ²	p-value
1	SSY	Max TWI	-	-	0.860	<0.05
2	SSY	DA	-	-	0.695	=0.05
3	SSY	$\Sigma\Delta z$	-	-	0.702	=0.05
4	SSY	Roughness	-	-	0.462	=0.05
5	SSY	Max Δz	-	-	0.756	>0.05
6	SSY	Max TWI	$\Sigma\Delta z$	-	0.883	>0.05
7	SSY	Max TWI	DA	-	0.888	>0.05
8	SSY	Max TWI	$\Sigma\Delta z$	DA	0.882	>0.05
9	SSY	Max TWI	$\Sigma\Delta z$	Roughness	0.864	>0.05

Table 4. The results of a selection of model runs. Green models indicate statistically significant p-values, yellow indicate inconclusive results, and red indicates poor statistical significance.

Based on the results of this analysis, it was decided that the top three models would be used to estimate mean annual SSY in the ungauged catchments delineated for this analysis. The topographic metrics used in the models for these four catchments are shown in Table 5.

Watershed	Max TWI	Drainage Area (m ²)	$\Sigma\Delta z$ (m)
Nostoc Creek	14.44	1919700	13580
Longer Creek	15.46	2640600	19091
Cold Creek	11.81	696600	4485
McRae Creek	16.59	15577914	15819

Table 5. Topographic metrics for predicting mean annual SSY in ungauged basins using linear models.

The results of the final model runs are shown below in Table 6. This shows the results of the modelling for the ungauged basins as well as the experimental watersheds.

Predictor →	Max TWI	Drainage Area	$\Sigma\Delta z$	
Watershed	Predicted SSY (t/km ²)	Predicted SSY (t/km ²)	Predicted SSY (t/km ²)	
Nostoc Creek	90.41	37.86	66.08	
Longer Creek	108.73	40.21	80.41	
Cold Creek	43.17	33.89	42.43	
McRae Creek	129.03	82.28	71.90	Actual Mean Annual SSY (t/km ²)
1	53.94	34.91	31.71	97.1
2	50.17	34.22	31.44	17.7
3	127.77	34.73	35.10	108.2
6	0.05	32.01	30.77	5.5
7	5.62	32.03	30.77	2.5
8	32.75	32.14	30.81	5.3
9	-15.75	31.85	30.77	3.3
10	-4.08	31.99	30.82	10.3
Mack	95.08	50.44	62.16	67.7
Lookout	203.40	234.56	230.61	231.3

Table 6. The results of the top three linear models. Model input data is shown on the far right for the experimental watersheds to compare results. Watersheds delineated as part of analysis are bolded.

It is clear from these results that topography alone is not enough to predict mean annual SSY in these small catchments. The models performed the best in the largest catchments, Mack and Lookout Creeks. In the smaller creeks the results were poor and variable. Max TWI, the strongest predictor in the models, overestimated some sites, underestimated others, and calculated negative SSY in the two smallest catchments. Drainage area and $\Sigma\Delta z$ both gave similar results for all small catchments. The poor results for the smallest catchments could be driven by many things. First, the data used to calculate SSY was calculated with the entire available record for all sediment data, which is different for every watershed. The lack of temporal synchronicity can skew results as short events can move a lot of sediment. The HJA has a history of large disturbance events that have moved significant quantities of sediment and restructured channels. The floods of 1964 and 1996 are examples of this (Goodman et al. 2023).

Another cause for potential error is the lack of a quantification of past harvesting and underlying bedrock. Multiple attempts were made to create a scale of relative difference between the sites, but the exercise failed to produce a good relationship with SSY.

The change analysis may still be a good measure of relative erosion rate in a catchment, but the addition of other information may also be needed to provide predictions of sediment yield. Discharge has a proven relationship with SSY, but not every catchment has gauging systems or the capital to invest in them. Potential error in this portion of the analysis could be driven by higher than assumed error in the bare earth DEMs derived from LiDAR in a heavily forested area. This would have led to a lot more uncertainty in the change values.

The results may also have been skewed by the range of catchment sizes used in the study. The ability for these metrics to perform well at predicting SSY in the larger catchments may mean that the model needs more data.

Lastly, we used a linear model for this analysis. Linear models, while powerful and easy to use, do not always perform well when working with complex interactions. More complex models that consider other functions and the inclusion of time series data would likely find more reliable predictors.

Conclusions

Predicting mean annual suspended sediment yield is complex. While LiDAR derived metrics of topography may be able to help make these predictions at large scales, small scale modeling remains challenging. Topography alone cannot predict the interactions occurring at the headwater scale that control sediment movement.

Topographic wetness index, drainage area, and our proxy measure of erosion rate were all able to explain the variance in our data using linear modelling. Topographic wetness index represents a measure of steady-state wetted surfaces and should be a good proxy in lieu of discharge data. We hypothesize that TWI is able to explain variance well because it relates to the amount of water flowing overland in a catchment. If a catchment has more water flowing over more material, this should result in a higher sediment yield.

Using change analysis between multiple aerial LiDAR acquisitions provided a measure of erosion rate that was also able to explain the spatial variability in mean annual SSY. not a strong predictor of SSY at all scales.

The promise of the results in the larger catchments could indicate a need for further research and the inclusion of geologic information and disturbance legacies to truly understand sediment flow in these steep volcanic catchments. Further analysis will be necessary with the possible including of a wider range of catchment types and the use of more complex modeling.

Next Steps

One thing worth note is that the old shapefiles of the experimental basins does not perfectly match up with the new stream network in every location. Noticeable variations exist in watersheds 6, 7, and 8. To correct this, we will first check further resampling resolutions between

20m and 30m to balance landscape resolution with road resolution for flow direction. This way, we might find a better resolution capable of being used to determine flow. The next step will be to visit the site and ground truth the layer in the field. If the new stream network is correct, we will need to then delineate the old experimental watersheds again to correct them.

My dissertation is focusing on understanding landscape/geology/streamflow interactions in the HJA. I am trying to understand water flow paths and catchment storage potential using water stable isotopes and other tracers. The metrics derived from this project will allow me to investigate storm response at the catchment scale as it relates to physiography. I will also use these metrics within Spatial Stream Network models to investigate drivers of spatial variability in isotope ratios in surface water.

Data Sources

Hydrologic Data: <https://andlter.forestry.oregonstate.edu/data/abstract.aspx?dbcode=HF004>

Utilized mean annual SSY as calculated by Bywater-Reyes et al., 2018. They utilized long term SSY data in the experimental watersheds and calculated mean annual values from the long term data. Samples are collected in composite three weeks samples at each watershed, in addition to sporadic storm samplings at various watersheds. All of the data was provided by the HJ Andrews Experimental Forest (Johnson, 2019).

LiDAR DEM Data: <https://andrewsforest.oregonstate.edu/data/aerial>

Titles – GI010 (2008 DEM) (Spies, 2016)

Data type: Raster

Projection: UTM Zone 10

Units: Meters

Resolution: 1m

We also have access to the 2020 DEM, though it is still in the process of being added to the database. It was created using the same projection and units as the 2008 DEM. The 2020 DEM created by David Bell (USFS).

Raster files provided for each DEM: Elevation, Slope, Aspect, Hillshade

References

1. Anderson, Scott, and John Pitlick. "Using Repeat Lidar to Estimate Sediment Transport in a Steep Stream." *Journal of Geophysical Research: Earth Surface* 119, no. 3 (2014): 621–43. <https://doi.org/10.1002/2013JF002933>.
2. Brooks, J. Renée, Parker J. Wigington Jr., Donald L. Phillips, Randy Comeleo, and Rob Coulombe. "Willamette River Basin Surface Water Isoscape ($\Delta^{18}\text{O}$ and $\Delta^2\text{H}$): Temporal Changes of Source Water within the River." *Ecosphere* 3, no. 5 (2012): art39. <https://doi.org/10.1890/ES11-00338.1>.
3. Bywater-Reyes, Sharon, Kevin D. Bladon, and Catalina Segura. "Relative Influence of Landscape Variables and Discharge on Suspended Sediment Yields in Temperate Mountain Catchments." *Water Resources Research* 54, no. 7 (July 2018): 5126–42. <https://doi.org/10.1029/2017WR021728>.
4. DeLong, S. B., M. N. Hammer, Z. T. Engle, E. M. Richard, A. J. Breckenridge, K. B. Gran, C. E. Jennings, and A. Jalobeanu. "Regional-Scale Landscape Response to an Extreme Precipitation Event From Repeat Lidar and Object-Based Image Analysis." *Earth and Space Science* 9, no. 12 (2022): e2022EA002420. <https://doi.org/10.1029/2022EA002420>.
5. Edson, Curtis, and Michael G. Wing. "LiDAR Elevation and DEM Errors in Forested Settings." *Modern Applied Science* 9, no. 2 (January 10, 2015): p139. <https://doi.org/10.5539/mas.v9n2p139>.

6. Goodman, Arianna C., Catalina Segura, Julia A. Jones, and Frederick J. Swanson. "Seventy Years of Watershed Response to Floods and Changing Forestry Practices in Western Oregon, USA." *Earth Surface Processes and Landforms* n/a, no. n/a. Accessed March 13, 2023. <https://doi.org/10.1002/esp.5537>.
7. Johnson, S.; Fredriksen, R. 2019. Stream chemistry concentrations and fluxes using proportional sampling in the Andrews Experimental Forest, 1968 to present. Long-Term Ecological Research. Forest Science Data Bank, Corvallis, OR. [Database]. Available: <http://andlter.forestry.oregonstate.edu/data/abstract.aspx?dbcode=CF002>. <https://doi.org/10.6073/pasta/bb935444378d112d9189556fd22a441d>. Accessed 2023-03-14.
8. Pavelsky, Tamlin M., and Laurence C. Smith. "Remote Sensing of Suspended Sediment Concentration, Flow Velocity, and Lake Recharge in the Peace-Athabasca Delta, Canada." *Water Resources Research* 45, no. 11 (2009). <https://doi.org/10.1029/2008WR007424>.
9. Spies, T. 2016. LiDAR data (August 2008) for the Andrews Experimental Forest and Willamette National Forest study areas. Long-Term Ecological Research. Forest Science Data Bank, Corvallis, OR. [Database]. Available: <http://andlter.forestry.oregonstate.edu/data/abstract.aspx?dbcode=GI010>. <https://doi.org/10.6073/pasta/c47128d6c63dff39ee48604ecc6fabfc>. Accessed 2023-03-14.
10. Swanson, F.J. 2013. Upper Blue River geology clipped to the Andrews Experimental Forest, 1991 ver 4. Environmental Data Initiative. <https://doi.org/10.6073/pasta/1c428e8798a2f3975f202636d3ad6139> (Accessed 2023-03-14).